Geomechanics and Engineering, *Vol. 29, No. 1 (2022) 65-77*
https://doi.org/10.12989/gae.2022.29.1.065

Application of cuttings to estimate the static characteristics of the dolomudstone rocks

Ahmad Rastegarnia[1], Mohammad Ghafoori*[1], Naser Hafezi Moghaddas[1], Gholam Reza Lashkaripour[1] and Hassan Shojaei[2]

[1]*Department of Geology, Faculty of Science, Ferdowsi University of Mashhad, Mashhad, Iran*
[2]*National Iranian Oil Company, South Oil Company, Ahvaz, Iran*

(Received November 6, 2021, Revised December 30, 2021, Accepted January 27, 2022)

Abstract. Determination of strength properties of intact rock using artificial cores has been considered in recent years. In this study, some relationships for estimating the static properties of dolomudstone cores of the Asmari reservoir were presented using artificial cores prepared from cuttings of two wells, southwest of Iran. For this purpose, first natural cuttings (NC) and 33 cores including dolomite limestone (dolomudstone), anhydrite and anhydrite dolomite were prepared between depths of 1714 and 2208 meters. Petrographic, physical, mechanical and dynamic tests were performed on cores, NC and artificial cuttings (AC) which was prepared from the residuals of dolomudstone cores. For preparing the artificial cores, the average porosity of the dolomudstone cores was considered and determined using four methods. Artificial and natural cuttings were classified as dolomite limestone and dolomite limestone to calcareous dolomite, respectively. Using ordinary Portland cement (OPC), water, AC and NC artificial cores were prepared. Results of evaluating the proposed relationships using statistical criteria showed that the static properties of the artificial cores can be used to predict the static properties of the dolomudstone cores.

Keywords: artificial and natural cores; natural and artificial drill cuttings; petrography; static parameters

1. Introduction

Considering the challenges of drilling of the wells and developing hydrocarbon fields, understanding the rock geomechanical properties to reduce the costs at the technical design of wells, development oil fields, enhanced oil recovery, and etc. is very vital and necessary (Moradi *et al.* 2018, Abd El-Aal *et al*. 2020, Yan *et al*. 2017, Singha and Chatterjee 2017, Xu *et al.* 2022). Due to the importance of static properties (uniaxial compressive strength (UCS) and elastic modulus (Es)) of the rocks, the results of some studies to estimate these properties using artificial cores are presented below. Tests such as single compressive strength test (Cheshomi and Sheshde 2013), static penetration test (Mateus *et al*. 2007) and continuous wave record test on cuttings (Nes *et al*. 2001) are the experiments that have been used to estimate the UCS using experiment on cuttings.

Amiri and Momivand (2018) assessed the relationship between UCS of artificial cores and the UCS of real sandstone samples with porosity between 9% and 35%. Fedrizzi *et al.* (2018) investigated the relationships between porosity, permeability, wave velocity and amount of synthetic cements of the carbonate samples and compared the results with the properties of natural carbonate cores. The relationships between the UCS of the real and reconstructed cores were assessed by Mehrabi Mazidi *et al*. (2012). Karaman and Bakhytzhan (2020) presented some relationships for estimating the UCS of the concrete using the properties of the parent rock. Wang *et al.* (2015) stated that dynamic modulus of synthetic carbonate cores increases with increasing secondary porosity and degree of saturation. Johansson *et al.* (2009) proposed a method using drill cuttings to investigate the homogeneity and heterogeneity of the bed rock. Ivan'kova and Bogoslovskii (2008) used drill cuttings to perform a petrophysical interpretation of the well-logging data in wells drilled in carbonate rocks. They stated that the cuttings collected from each well section reflect the composition and properties of the studied sections and significantly overlap with the raw rock material crushed by the drilling bit. Li *et al.* (2015) investigated the influence of cementation factors on engineering properties of the artificial cores with porosity between 50% and 70%. Lee *et al.* (2008) studied strength characteristics of the artificial granite specimens. Boggs and Boggs (2009) stated that the gradation of the fillers has a great influence on the properties of artificial cores.

In current research, first, petrographic and geomechanical characteristics of the cuttings and 33 cores such as dolomite limestone (21 cores), anhydrite (7 cores) and anhydrite dolomite (5 cores) were investigated. Then, UCS and Es of the real dolomite limestone cores were estimated based on UCS and Es of the artificial cores prepared from the natural and artificial cuttings at wells 122 and 158 in the Bibi Hakimeh oil field, in southern Iran.

2. Study area

The Bibi Hakimeh oil field is located in Kohgiluyeh and Boyer-Ahmad provinces, south of Iran. This field consists of the Asmari reservoirs with a thickness of about 487

*Corresponding author, Professor
E-mail: ghafoori@um.ac.ir

ISSN: 2005-307X (Print), 2092-6219 (Online)

Fig. 1 Vp and Vs measuring device used in this study

meters, the Bangestan (Sarvak and Ilam formations) and the Khami (Fahlian, Gadvan and Darian formations). Present study was performed on 33 core specimens obtained from the Asmari formation at wells 122 and 158. Geologically, this field is situated at the east of Dezful Embayment in the Zagros sedimentary basin, in southwestern part of Iran.

3. Material and methods

3.1 Physical, mechanical and dynamic tests on real cores

In this study, 33 core specimens with height of 7.4 centimeters and diameter of 3.7 centimeters without any joint, crack and stylolite structures were prepared between depths of 1714 m and 2208 m in wells 122 and 158 of the Asmari reservoir at the Bibi Hakimeh oil field.

The results of petrographic tests (Section 4.1) showed that these 33 samples included 21 samples of dolomudstone (dolomite limestone), 7 anhydrite cores and 5 anhydrite dolomite cores. The top and bottom of the cores were straightened before the tests. Experiments to determine physical, mechanical and dynamic properties were performed on the samples. Before the mechanical tests, ultrasonic experiments were conducted on the samples to measure the shear and compressional wave velocities (Vs and Vp, respectively) according to the ISRM standard. The frequency used in these tests is 0.5 MHz. Fig. 1 shows an image of Vp and Vs measuring device.

Uniaxial compressive strength (UCS) test was performed according to the relevant standard and with loading rate of 0.7 MPa/s on the specimens (ASTM, 2002). Physical tests such as density (ρ), porosity (n), and water absorption (W_a) by weight were conducted according to the relevant standard.

Using saturation-immersion (SI) and helium porosimeter methods, the porosity of the specimens was measured. In helium method, using Boil-Mariot's law, in constant temperature conditions, the grain's volume is calculated as follow

$$P_1 V_1 = P_F (V_1 + V_2 - V_{grains}) \quad (1)$$

Finally, the specimen porosity is calculated using Eq. (2)

$$\phi = \frac{V_{total} - V_{grains}}{V_{total}} \quad (2)$$

This method only can calculate the effective porosity. Lack of adsorption process on the sample surface and rapid diffusion into the specimen pores considered as the advantages of this gas.

In calcimetery test, 30 grams of powder from each sample were poured into 30% hydrochloric acid solution for 24 hours. For specimens with dolomite impurities warming is required. After test, the residues were dried in the oven. The carbonate content equals to the weight difference in before and after test. The average of calcium carbonate of the dolomite limestone samples is presented in Table 2.

3.2 Making artificial cores

The cuttings used to prepare artificial cores must have the same gradation. Also, the porosity of the artificial cores must be placed into the porosity ranges of the real cores. For this purpose, 64 artificial cores were made using natural and artificial cuttings in laboratory. Finally, 42 artificial cores of them with porosity values in the range of porosity of the real cores were selected. In this study, two types of artificial cores were prepared. Artificial cores obtained from artificial and natural cuttings. Artificial cuttings were prepared from the residues of dolomite limestone cores and natural cuttings were collected during drilling of the wells. For preparing artificial cores, the artificial cuttings between sieve number 100 and 1.2 and natural cuttings between 10 and 100 sieves were selected. The weight percentages of aggregates, ordinary Portland cement (OPC) and water for the preparation of the mixture were 68%, 20% and 12%, respectively.

Water to cement ratio of 0.60 and OPC value were the same for all samples. After preparing the mixture, the mixture was poured into the molds. The molds were opened after 24 hours of initial setting and the cylindrical specimens were taken out and kept at the room temperature for 21 days. During the processing of the samples, the samples was wet one meal a day and their surfaces were covered with cloth. The characteristics of used OPC are presented in Table 1.

The experiments were performed on the artificial cores at natural moisture after 3 weeks. Before the UCS tests, bottom and top of the cylindrical specimens were smoothed by a machine and cores with height of 7.4 cm and diameter of 3.7 cm were prepared.

4. Results and discussion

4.1 Petrography of the samples

In present study, totally, 220 microscopic sections from wells 122 and 158 of the BH oil field were investigated (some samples in Fig. 2). In order to identify dolomite from calcite, a number of samples were stained with Alizarin red.

Table 1 Specifications of OPC used to prepare artificial cores

Blaine (cm^2/g)	Vicat test (min)	Free CaO%	Insoluble residue%	Al_2O_3%	SO_3%	LOI%	Fe_2O_3%	CaO%	MgO%	SiO_2%
3000	131-252	0.58	0.36	4.36	3.10	0.56	4.01	63.21	2.75	20.69

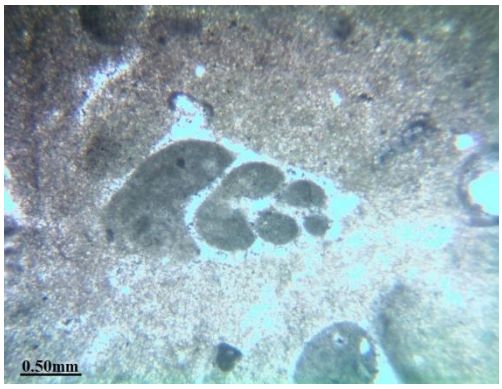

(a) Bioclastic wackestone contains gastropod fossil

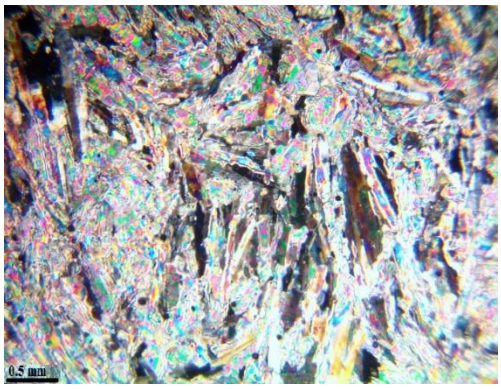

(b) Anhydrite

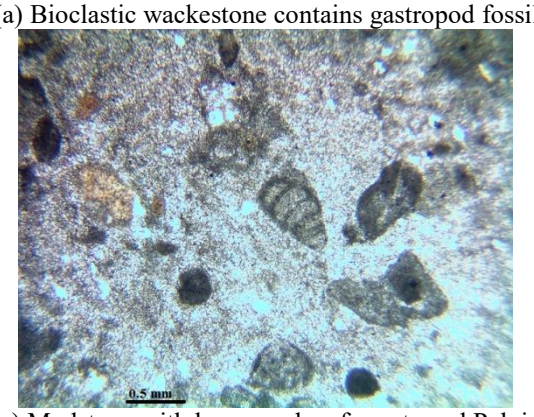

(c) Mudstone with low crumbs of quartz and Peloid

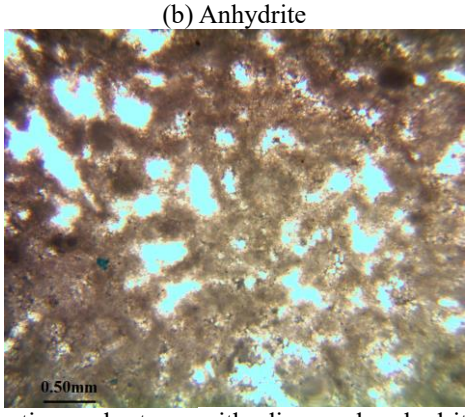

(d) Bioclastic wackestone with dispersed anhydrite (severe dolomitization)

Fig. 2 Some of the thin sections from wells 122 and 158

Dolomitization (Fig. 2(d)) and anhydrite cementation are among the common processes in the Asmari limestone formation, as a laminate and filler between the crystalline and hollow space (Fig. 2(d)). Based on microscopic sections, the carbonate cores are composed of calcite, dolomite, quartz, anhydrite, and iron oxides and hydroxides. More than 50% of the minerals that make up the cores are calcite and a significant amount of dolomite (Fig. 2). The samples in the studied wells contain foraminiferal and gastropod fossils (Fig. 2). Carbonate specimens were classified as dolomudstone and dolowackestone (Embry and klovan 1971, Dunham 1962). The dolomudstone cores were used to produce artificial cuttings.

To determine the type and phase percentage of minerals forming the samples, X-ray diffraction (XRD) with copper Kα beam with wavelength, λ = 1.5406Å was used. XRD analyzes were performed in the range of 2θ angle of 2 to 60 degrees on a powder sample with a size of 50 microns, step size of 0.05 and a duration of 5 hours. XRD results of a sample of artificial cuttings of the dolomite limestone cores (dolomudstone) is presented in Fig. 3 (Fig. 3-upper part). Because of presence of very small of montmorillonite clay, it can be expected that the swelling potential of the samples is low. Physical tests showed that water absorption (Wa) of the specimens (4.04%) was also low (Table 2).

The range of dolomite mineral in dolomite limestone samples varies from 20% to 40%. The percentage of anhydrite, calcite and quartz minerals in anhydrite dolomite sample are 20, 15 and 5%, respectively.

The lithology of natural cuttings (NC) was categorized as dolomite limestone to calcareous dolomite with impurities of gypsum, quartz, clinochlore, calcium montmorillonite and vermiculite. The amount of impurities in the natural cuttings was more than artificial cuttings (AC). XRD results of two samples of the drill cuttings prepared from these two wells (i.e., natural cuttings) are also presented in Fig. 3-lower part. Mixed-layer clay minerals of natural cuttings are chlorite-montmorillonite type. There is also a small amount of glauconite in these wells.

The XRD results of two examples of anhydrite and anhydrite dolomite cores are presented in Fig. 4.

Fig. 5 shows the scanning electron microscope (SEM) and energy dispersive spectroscopy (EDS) results of an anhydrite specimen. The SEM images of dolomite limestone specimens are also presented in Figs. 7 and 8. For

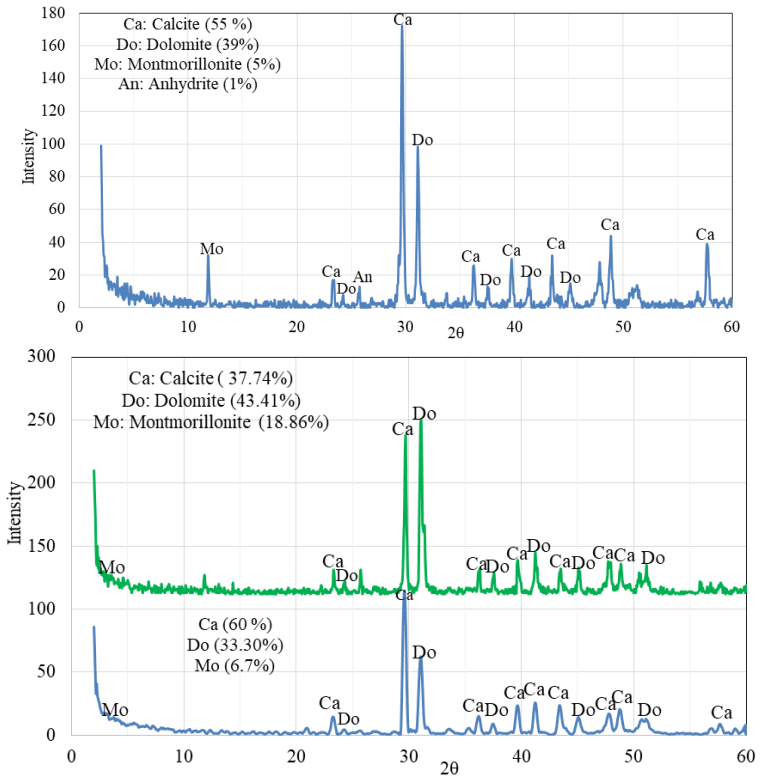

Fig. 3 XRD diagram of artificial (upper part) and natural (lower part) cuttings

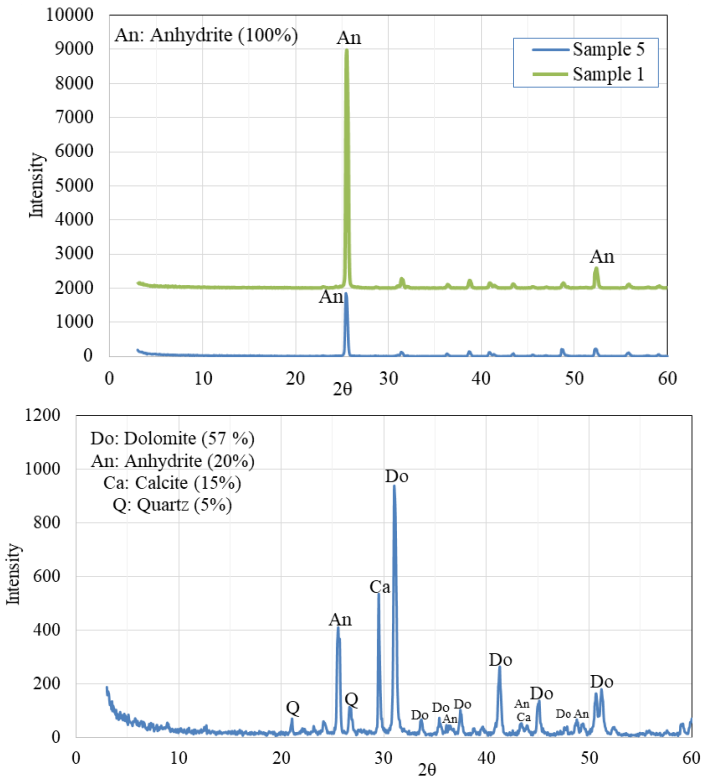

Fig. 4 The XRD results of anhydrite (top part) and anhydritic dolomite (bottom part)

SEM microscopic analysis, small fragments of rock samples with a diameter of 20 mm were selected. Because the samples are not electronically conductive, the thin composite layer of gold-palladium was coated before the SEM equipment was run.

In addition to the SEM, thin sections and XRD results, the weight of rock powder of the anhydrite samples after calcimetery test (described in section 3.3.5) was higher than

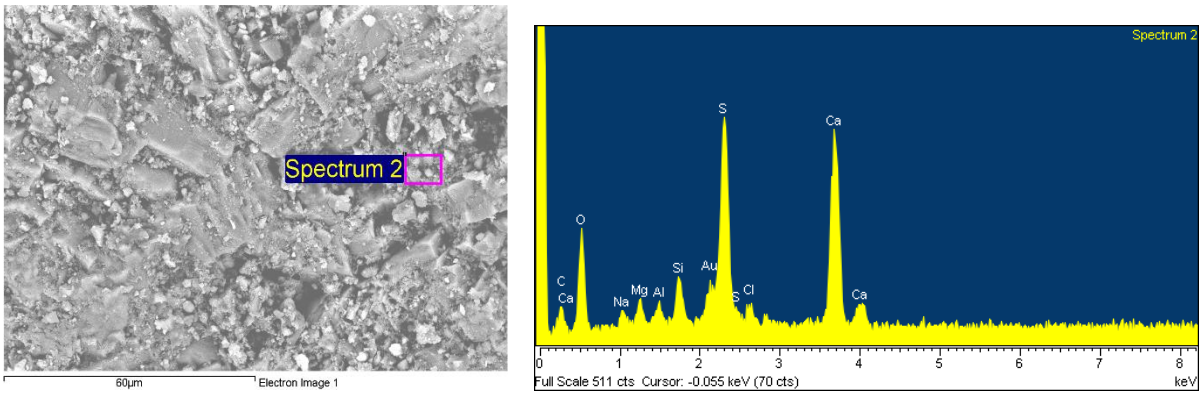

Fig. 5 The SEM and EDS of an anhydrite sample

Table 2 Characteristics of the studied cores

Lithology	S.N.	Statistic	UCS (MPa)	Es (GPa)	V_p (Km/s)	V_s (Km/s)	ρ (g/cm^3)	n (%) using SI method	Wa (%)	$CaCO_3$ (%)
Dolomite limestone	21	Min.	50.91	14.00	4.51	2.63	2.42	0.56	0.06	42.00
		Max.	110.0	26.00	5.81	3.46	2.67	6.50	4.04	77.00
		Mean	74.06	17.51	5.20	3.19	2.65	3.07	1.34	61.68
Anhydrite	7	Min.	28.2	3	5.1	2.80	2.84	2.8	0.08	-
		Max.	40	8	5.7	3.20	2.87	3.5	3.04	-
		Mean	32	5	5.42	3.00	2.86	3.02	1.34	-
Anhydrite dolomite	5	Min.	46	5	4.9	2.65	2.5	2.19	0.05	-
		Max.	65	12	5.94	3.4	2.75	3.1	2.8	-
		Mean	57	8.85	5.48	3.10	2.65	2.91	1.2	-

before this test due to the water absorption. This means that the anhydrite samples absorbs water and converted to the gypsum. Gypsum mineral ($CaSO_4$. $2H_2O$) converts to basanite mineral ($CaSO_4$. $0.5H_2O$) at 70°C with loss of water and converts to anhydrite mineral with increasing temperature up to 95°C and loses all its water (Klein and Hurlbut 1985).

4.2 Results of physical, mechanical and dynamic tests on the cores

Results of experiments such as density (ρ), porosity (n), water absorption (W_a), calcimetery, UCS, Vp and Vs on 33 cores such as dolomite limestones, anhydrite and dolomite anhydrite are presented in Table 2. The Vs of dolomite limestone samples (dolomudstone) is in the range of 2.63 to 3.46 km / s. Table 2 shows that the average UCS and Es are 74.06 MPa and 17.51 GPa, respectively. Also, the average porosity using SI method is equal to 3.07%. Cuttings obtained from dolomite limestone cores were used to prepare the artificial cuttings.

4.3 Porosity estimation of the dolomite limestone cores using image processing method

The porosity of artificial cores should be selected within the range of porosity of the real cores. For this purpose, the porosity of real samples was investigated by different methods. Then the average values of the four methods were used to select the artificial cores. In this study, image processing using ImageJ and microstructural image processing (MIP) software were used to determine the porosity of the samples. The MIP version used in the present study is MIP4 Students (Nahamin Pardazan Asia Co., Iran, available on: http://metsofts.ir/download-mipstudent/). Image processing determines the percentage of phases, number and size of particles, area, perimeter, diameter, circularity, and other geometric characteristics of the grains. Grain size estimation is usually conducted using image analysis methods by measuring the minimum Feret diameter ($d_{Fmin.}$) and maximum Feret diameter ($d_{Fmax.}$). The $d_{Fmax.}$ and $d_{Fmin.}$ are the largest and smallest possible distance between two parallel planes which are surrounded the particle. One way to improve image quality is to remove noise from the image. Noise in the image includes light and dark spots and abnormalities that are randomly distributed on the image. In this study, the median filter is used to smooth the image and eliminate possible noise in the image. Grain and background were separated by the threshold command. Also, the watershed algorithm was used to separate the grains. The steps of image processing and extracting geometric properties on SEM images using ImageJ software are presented in Fig. 6. An image of the threshold command is shown in Fig. 7. An example to determine the porosity based on a SEM image using MIP software is provided in the Fig. 8.

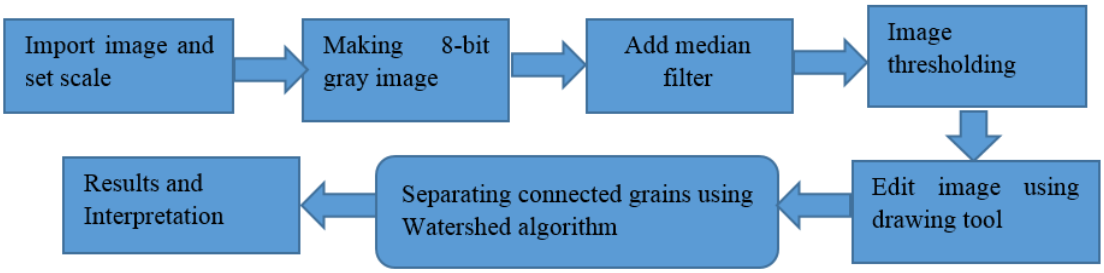

Fig. 6 Image processing flow chart used in this study

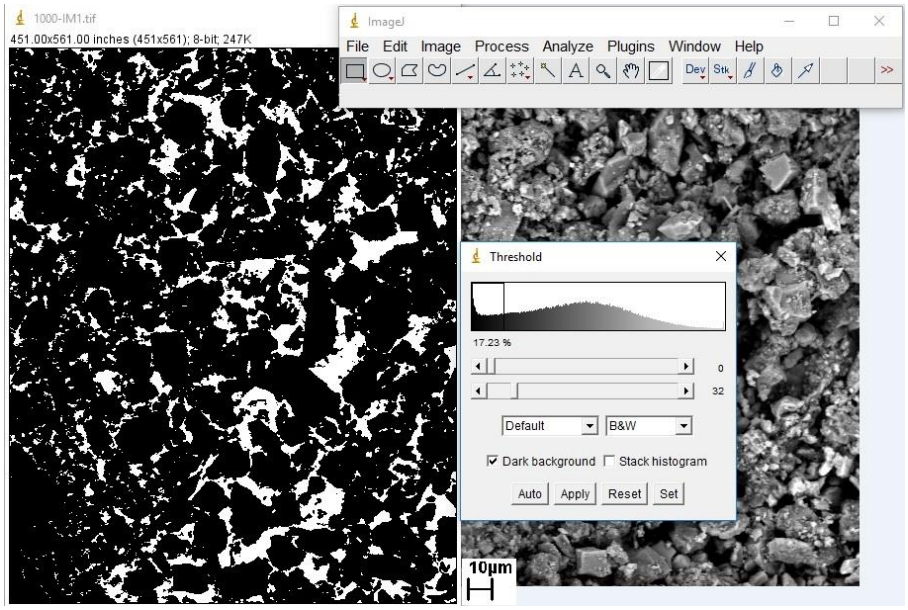

Fig. 7 An example of a raw image (right) and running the Threshold command (left) in ImageJ

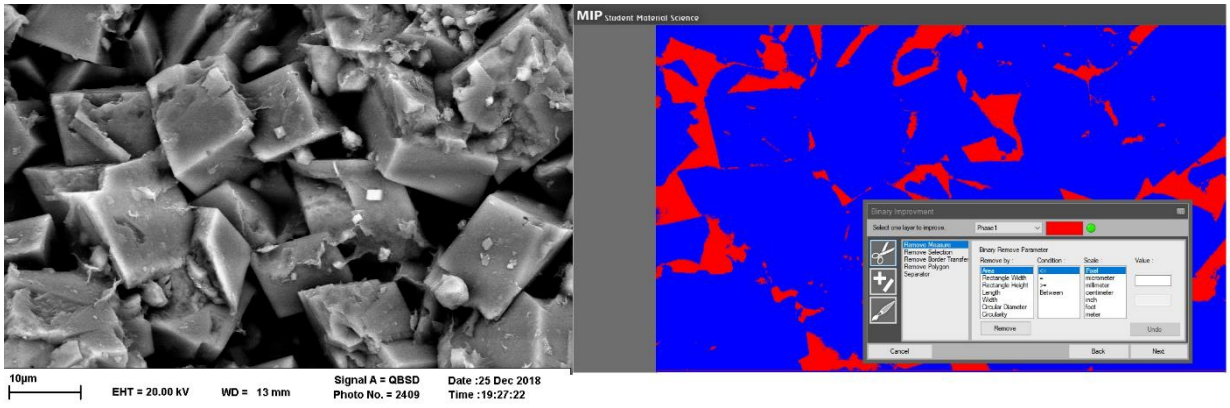

Fig. 8 An example of determination the percentage of porosity with MIP software - left) SEM raw image and right) determination the phase of cavities

The porosity of the dolomite limestone cores was determined using MIP and ImageJ software and compared with saturation-immersing (SI) and helium methods (Fig. 9). Results show that the software methods of determining porosity based on the SEM images show the highest amount and the SI method shows the lowest amount of porosity (Fig. 9). The helium method also displays a greater amount than the SI method because of better and faster penetration of gas particles into the rock pores.

4.4 Gradation and standard compaction tests on the cuttings

Cuttings were graded according to the ASTM standard. Fig. 10 shows an images of the cuttings. Gradation of the artificial cores must be selected the same size as gradation of rock cores. Due to the diversity of gradation of aggregates produced from primary rock in terms of shape and geometric dimensions and to equalize the amount of

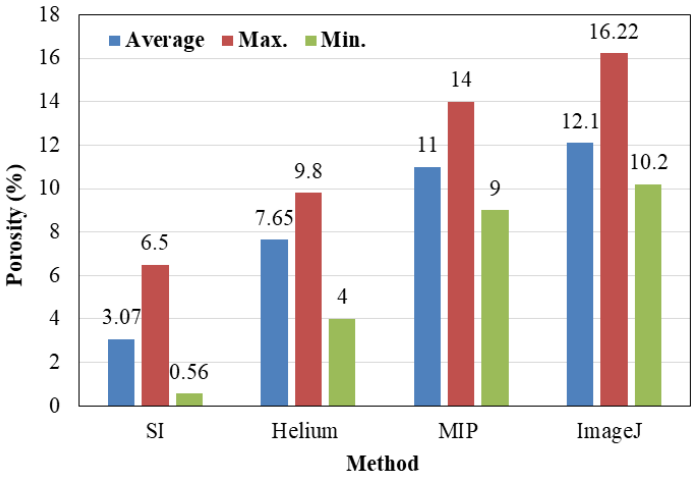

Fig. 9 Comparison of porosity of dolomite limestone cores using different methods

Fig. 10 Examples of cuttings: right) artificial cuttings and left) natural cuttings

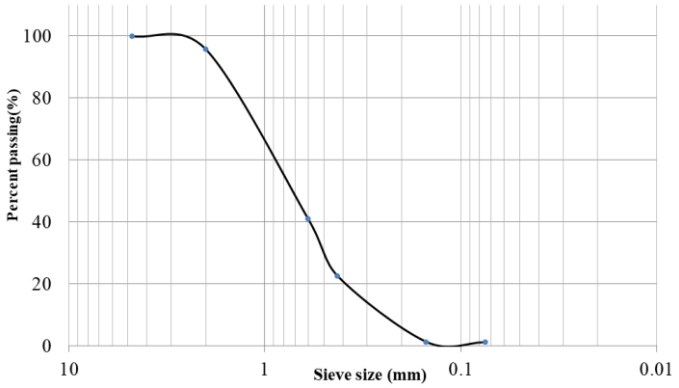

Fig. 11 An example of gradation curve of natural cuttings

Table 3 The C and φ of the cuttings using direct shear test

Cuttings	Saturated density (g/cm^3)	Dry density (g/cm^3)	σ_n (kg/cm^2)	τ (kg/cm^2)	C (kg/cm^2)	Phi (degree)
Natural cutting	2.31	2. 22	0.5	0.05	0.010	4.6
			1	0.091		
			1.5	0.13		
Artificial cutting	2.47	2.4	0.5	0.14	0.033	17.23
			1	0.24		
			1.5	0.45		

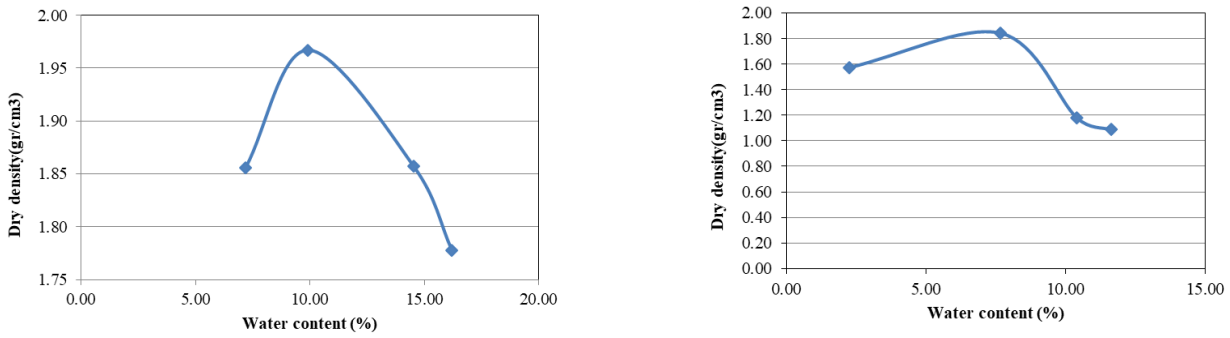

Fig. 12 Examples of compaction curve (left – natural cuttings and right- artificial cuttings)

Fig. 13 Sample images after direct shear test (the direction of the arrowheads shows the direction of shear surface): natural cuttings (left side) and artificial cuttings (right side)

porosity in them, it is necessary to select a same grain size distribution curve of artificial core samples and mixed with the same ratio of water to cement. Thus, the compositional properties of the prepared artificial cores are uniform and the only variable factor in them is the lithology of aggregates. The grain size distribution curve of artificial and natural cuttings was used according to Figs. 11 and 12. In order to equalize the porosity of the artificial and real cores, 64 artificial cores were made and among them, 42 cores with porosity in the ranges of porosity of real cores were selected for performing the UCS test.

Natural cuttings have an average of uniformity coefficient (Cu) and curvature coefficient (Cc) of 12.3 and 1.51, respectively. In all samples, the amount of fines (passing through the sieve of 200) is less than 5%. Also, all samples of natural cuttings passed through the sieve number of 10. The natural cuttings classified as well graded sand (SW) based on unified classification system (Fig. 12). Fig. 17 shows an example of a gradation curve of the artificial cuttings. On 18 samples of artificial cuttings, the average of Cu and C_C were determined to be12.27 and 2.57, respectively. In all samples, the percent passing of sieve of 200 and sieve of 4 is less than 5% and 50%, respectively. Hence, the gradation of artificial cuttings classified as well graded gravel (GW) based on unified classification system.

4.6 Los Angeles and impact value tests on artificial cuttings

In this study, the amount of weight loss due to the abrasion using the Los Angeles machine which is done for gravel materials after 500 cycles according to the ASTM standard has been determined (ASTM, 2006). The results of this experiment and the impact value are given in the Table 4. As can be seen, based on the results of the Los Angeles test, samples of dolomite limestone in the Bibi Hakimeh field have an average weight loss of 28% (Table 4).

Abrasion effect on gradation curve of artificial cuttings is displayed in Fig. 17. This figure shows that the abrasion is greater in a certain range of grain size. For smaller particles, the abrasion is greater than coarse particles, which may be related to the particle lithology or the gradation effect.

The cuttings resistance is measured using aggregate impact value (AIV) test. This test is standardized by the British Standard (BC 812, 1989). In this test, dolomite limestone aggregates were first sieved using 12.5 and 10 mm sieves and the remaining materials between these two sieves were selected. Then the materials in three layers and each layer with 25 blows are poured into a cylindrical container. Using a metal mallet, 15 times from a height of 380 mm blows are applied to the aggregates in a free fall state. Finally, after the impacts, the weight of the parts of the aggregates that passes through the sieve number 8 is determined and the impact value is calculated. In this research, the AIV of the artificial cuttings of dolomite limestone has been determined (Table 4). The AIV and Los Angeles tests were not performed on the natural cuttings (NC) because all of these cuttings passed through the sieve number 10 (size 2 mm).

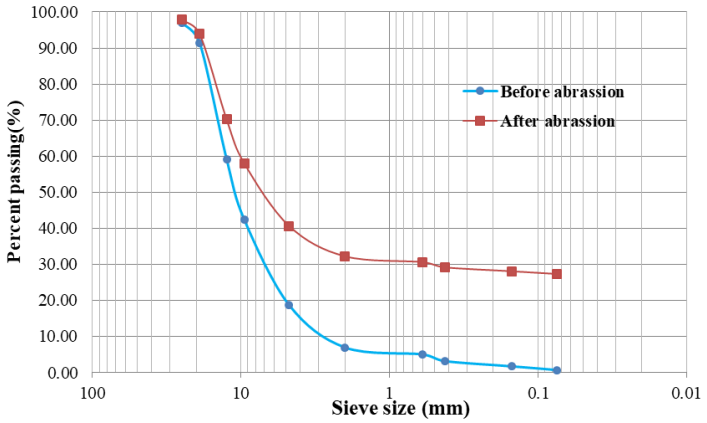

Fig. 14 The effect of abrasion on the gradation curve for one of the samples

(a) Molds used to make artificial cores

(b) A sample of prepared artificial cores

(c) A core prepared from artificial cuttings after UCS tes

(d) A core prepared from natural cuttings after UCS test

Fig. 15 Preparation and testing of UCS on artificial cores

Table 4 The results of AIV and Los Angeles tests

Parameters	Min.	Max.	Mean	Standard deviation	Variance
AIV	3	17	11.06	4.461	19.90
Los Angeles	7	44	27.93	11.709	137.11

4.7 Results of experiments on artificial cores

A set of physical and mechanical tests were performed on the 42 artificial cores according to the related standards to compare the engineering properties of the dolomite limestone and artificial cores. These tests include determining the physical properties, uniaxial compressive strength test, and SEM images of the fractured specimens.

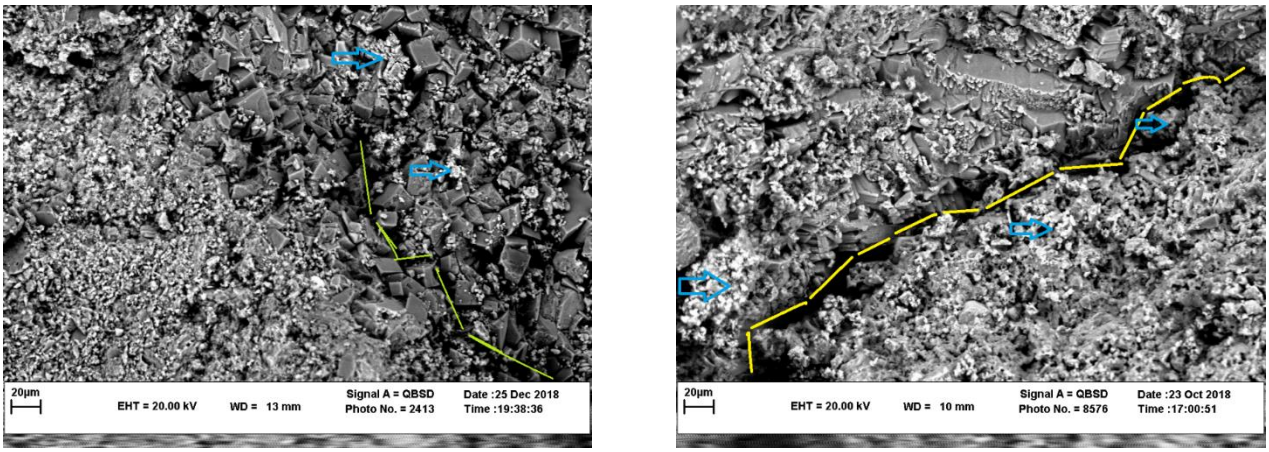

Fig. 16 The SEM images of artificial core made of natural (left) and artificial (right) cuttings after UCS test

Table 5 Results on 21 artificial cores prepared from AC

Statistics	UCS (MPa)	Es (GPa)	Wa (%)	n (%)	Density (g/cm^3)
Min.	19	0.21	4	6.20	2.2
Max.	34	1.10	15	14.1	2.58
Mean	25.51	0.46	10.96	8.06	2.39

Table 6 Results on 21 artificial cores prepared from NC

Statistics	UCS (MPa)	Es (GPa)	Wa (%)	n (%)	Density (g/cm^3)
Min.	11	0.09	5.24	7.8	1.83
Max.	19.3	0.93	20.10	16.5	2.52
Mean	15.65	0.42	14.73	9.01	2.23

Physical and mechanical test results on 21 artificial cores obtained from cuttings of dolomudstone are presented in Table 3. Results of UCS test on three core samples made of pure cement showed an average, minimum and maximum strength of 15 MPa, 14MPa and 16 MPa, respectively. Fig. 15 shows examples of cores in the UCS test.

Based on physical and mechanical tests performed on dolomudstone cores (Table 2) and artificial cores (Table 5), the uniaxial compressive strength of the dolomudstone cores is between 50.91 MPa and 110 MPa. Also, the UCS for artificial cores prepared from AC varies between 19 MPa and 34 MPa. The Es of the dolomudstone cores varies between 14 GPa and 26 GPa (Table 2) and Es of artificial cores prepared from AC varies between 0.21 GPa and 1.1 GPa (Table 5). The results of artificial cores made from natural cuttings (NC) are also shown in Table 6.

Water to cement ratio, the amount of cement used for each sample, and gradation curves in both artificial and natural cuttings were selected the same. Artificial and natural cuttings were classified as well graded gravel and well graded sand, respectively. The lithology of the artificial cuttings is dolomite limestone, whereas the lithology of the natural cuttings is dolomite limestone to calcareous dolomite. As a result, the lithology, size (sand or gravel) and shape of the aggregates (rounded or angled) affects the UCS and Es of the artificial cores. Impurities in aggregates reduce the strength of artificial cores (Etemadi *et al.* 2020; Lerman *et al*. 2021). Artificial cores prepared from artificial cuttings more resistant than artificial cores prepared from natural cuttings. Because the roughness and interlocking of the artificial cuttings greater than natural cuttings. Increasing the surface roughness of the grains leads to increasing the strength properties (Wang *et al.* 2020, Abetua and Kebedeb 2021).

4.8 SEM images of crushed specimens at UCS test

To assess the penetration of cement into the aggregates in the artificial cores and compare with the samples of natural cores, SEM images were used. Examples of images taken from the broken cores are shown in Fig. 16. Cement particles (blue arrows) are visible between the grains. In this Fig., cracks (yellow lines) are visible between the boundaries of grain and cement particles.

4.9 Relationships between static parameters of dolomudstone cores and artificial cores

To determine the relationships among the parameters using the regression analysis, the equation of the best fit was determined at the 95% confidence interval. The coefficient of determination (R^2), root mean square error (RMSE), adjusted determination coefficient and the results of analysis of variance (ANOVA) were widely used to evaluate performance of empirical relationships (Fang *et al.* 2021, Huang *et al.* 2022, Zhang *et al.* 2021, Tilaki *et al.* 2020, Gholami *et al.* 2020). In current study, the relationships with the highest accuracy were also presented (Table 7). It is observed that the method presented in this study to predict the static properties of the cores using artificial cores prepared from the artificial cuttings (UCS_{AC}), has a coefficient of determination of 0.77. Relationship type based on the best correlation is of the second degree polynomial type (Table 7). The relationship between UCS of the dolomudstone cores and the Es of the artificial cores prepared from the artificial cuttings (Es_{AC}) also has a high accuracy (R^2= 0.72). As can be seen, in this study, a

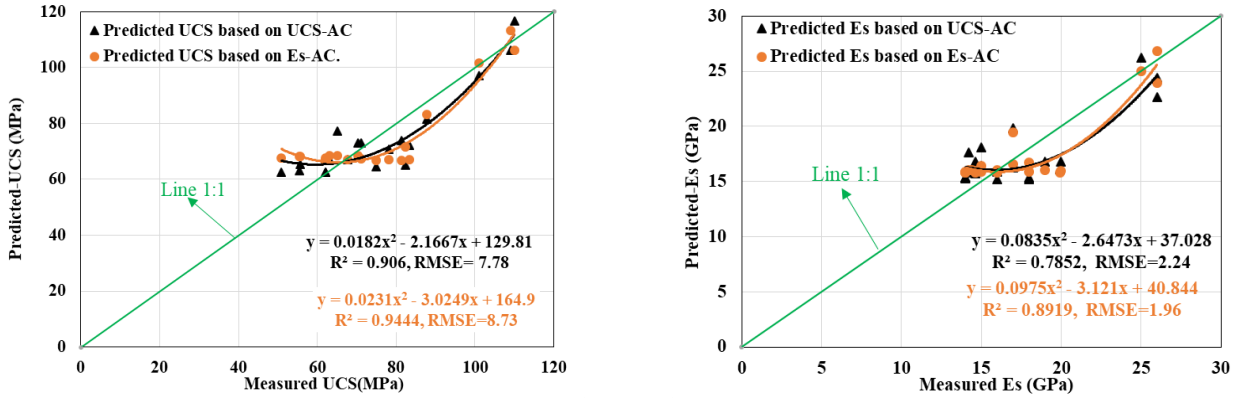

Fig. 17 Relationships between measured UCS of the dolomudstone cores and the estimated from artificial cores

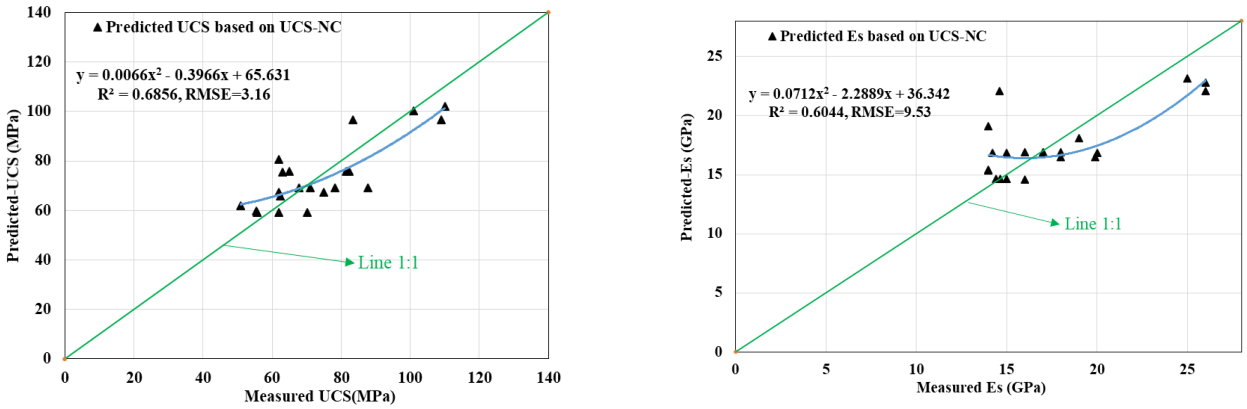

Fig. 18 Relationship between static parameters measured from real cores and predicted from artificial cores

Table 7 Relationships between static parameters of 21 dolomudstone cores and static parameters of cores made of artificial cutting (AC) and natural cutting (NC)

Equation		R^2	RMSE	R^2-adjusted	ANOVA F	ANOVA Sig.
$UCS = 0.5589(UCS_{AC})^2 - 26.987(UCS_{AC}) + 388.23$	(3)	0.77	13.96	0.76	31.42	0.00
$UCS = 84.756(Es_{AC})^2 - 60.82(Es_{AC}) + 77.636$	(4)	0.72	21.80	0.71	23.10	0.00
$UCS = 2.1334(UCS_{NC})^2 - 63.167(UCS_{NC}) + 526.51$	(5)	0.67	17.10	0.66	17.95	0.00
$Es = 0.0853(UCS_{AC})^2 - 3.8563(UCS_{AC}) + 58.734$	(6)	0.65	2.10	0.64	17.20	0.00
$Es = 22.143(Es_{AC})^2 - 17.497(Es_{AC}) + 19.264$	(7)	0.74	1.80	0.73	25.09	0.00
$Es = 0.3771(UCS_{NC})^2 - 10.95(UCS_{NC}) + 94.024$	(8)	0.50	2.26	0.49	8.89	0.00

significant relationship with high accuracy ($R^2 = 0.74$) has been obtained to estimate the Es of the dolomudstone cores based on the Es of the artificial cores made of artificial cuttings (Es_{AC}) (Table 7). The relationship between static parameters of the dolomudstone cores and UCS of artificial cores prepared from natural cuttings is also presented in this table.

Due to the weakness of the cores made of natural cuttings, it was not possible to record different strains in the UCS test for most samples. As a result, correlation of Es of the artificial cores obtained from natural cuttings (Es_{NC}) and the static properties of the dolomudstone cores was not investigated. Only the average values of some samples (0.42 GPa) are presented in Table 6. The relationship between UCS of artificial cores and UCS of dolomudstone cores shows the most accuracy because of the same lithology.

4.10 Evaluation of the presented relationships and comparison with previous researches

Table 8 Mean values of the predicted and measured static properties

Method	UCS (MPa) using NC	UCS (MPa) using AC	Es(GPa) using NC	Es (GPa) using AC
Predicted based on artificial cores	74.04	74.06	17.49	17.50
Measured based on real cores	74.06		17.51	

The relationships 3 to 8 were evaluated using RMSE and R^2. Fig. 17 shows the relationship of the estimated parameters based on the results of artificial cores with the measured values on real cores.

The relationships between UCS of real cores and UCS from reconstructed cores were assessed by Mehrabi Mazidi *et al.* (2012). They stated that the UCS values predicted by the linear and nonlinear methods provide lower values than the actual value and the UCS values predicted by the nonlinear method are closer to the real values.

Fig. 18 shows the relationship between measured UCS and Es of 21 dolomudstone cores with the predicted values of 21 artificial cores prepared from natural cuttings. It is observed that the relationship between measured UCS from real cores and predicted UCS from artificial cores has a high accuracy.

The average value of the predicted static properties based on 42 artificial cores with the average of measured value for 21 real cores is presented in Table 8. It is observed that the artificial cuttings for estimating the static properties of the real core is better than the natural cuttings. Also, the values of static properties estimated from artificial cores are equal or less than the measured values, which indicates the conservatism of the proposed method for estimating the static properties dolomudstone cores.

5. Conclusions

In this study, petrographic, physical, mechanical and dynamic properties of 33 core specimens such as dolomite limestone, anhydrite and anhydrite dolomite between the depths of 1714 m and 2207 m in the wells 122 and 158 at the Bibi Hakimeh oil field, in southern Iran, were assessed. After examining the properties of the cores, the residuals of the dolomite limestone (dolomudstone) cores were crushed and artificial cuttings were prepared. Natural cuttings were also prepared from depths of 1714 to 2207 meters from these two wells. Petrographic (SEM and XRD), abrasion, gradation; standard compaction, direct shear, and physical tests were performed on the cuttings. The results showed that the strength properties of artificial cuttings were larger than strength characteristics of the natural cuttings.

The results of porosity determination of the dolomite limestone cores using saturation-immersion (SI), helium, and image processing methods showed that the image processing methods have the highest value and the SI method has the lowest porosity. Helium method also showed higher porosity than SI method due to the faster penetration of gas particles into the sample pores.

Statistical relationships for estimating UCS and Es of the real cores were determined based on the static parameters of artificial cores. The accuracy of the relationships based on R^2 and RMSE showed that it is possible to estimate the Es and UCS using artificial cores. Estimation of UCS of the real cores based on UCS of the artificial cores prepared from the artificial cuttings showed the highest accuracy. Also, significant relationships with high accuracy were obtained to estimate the Es of the cores based on the Es of the artificial cores. The values of static properties estimated from artificial cores were equal or less than the measured values. This indicates the conservatism of the proposed method for estimating the static properties.

Acknowledgements

Funding and necessary information for providing this work has been supported by the National Iranian South Oil Company (NISOC) and Ferdowsi University of Mashhad under grant number 43102 (12/02/1396), for which the authors are grateful.

References

Abd El-Aal, A.K., Salah, M.K. and Khalifa, M.A. (2020), "Acoustic and strength characterization of Upper Cretaceous dolostones from the Bahariya Oasis, Western Desert, Egypt: The impact of porosity and diagenesis", *J. Petrol. Sci. Eng.*, **187**, 106798. https://doi.org/10.1016/j.petrol.2019.106798.

Abetu, A.G. and Kebede, A.B. (2021), "Crushed concrete as adsorptive material for removal of phosphate ions from aqueous solutions", *WCM*, **2**(5), 40-46. https://doi: 10.26480/wcm.02.2021.51.57.

Amiri, M. And Momivand, H. (2018), "Making artificial sandstone with a wide range of porosity", *J. p. G.*, **2**(1), spring and summer of 2018 (in Persian)

ASTM C131-06 (2006), *Standard Test Method for Resistance to Degradation of Small-Size Coarse Aggregate by Abrasion and Impact in the Los Angeles Machine*.

ASTM D2938 (2002), *Standard Test Method for Unconfined Compressive Strength of Intact Rock Core Specimens, ASTM International*, Pennsylvania, U.S.A. https://doi.org/10.1520/D2938-95R02.

Boggs, J.R. and Boggs, S. (2009), *Petrology of Sedimentary Rocks*, Cambridge University press, Cambridge.

British Standard Institution, (1989), "*Code of Practice for Determination of Aggregate*", Impact Value, "B.S. 812"

Cheshomi, A. and Sheshde, E.A. (2013), "Determination of uniaxial compressive strength of microcrystalline limestone using single particles load test". *J. Petrol. Sci. Eng.*, **111**, 121-126. https://doi.org/10.1016/j.petrol.2013.10.015.

Dunham, R. (1962), "*Classification of Carbonate Rocks According to Depositional Textures*", Tulsa, Okla., American Association

of Petroleum Geologists.

Embry, A.F. and Klovan, JE. (1971), "A late Devonian reef tract on northeastern Banks Island, NWT", *Bull. Can. Petrol. Geol*., **19**(4), 730-781. https://doi.org/10.35767/gscpgbull.19.4.730.

Etemadi, M., Pouraghajan, M. and Gharavi, H. (2020) "Investigating the effect of rubber powder and nano silica on the durability and strength characteristics of geopolymeric concretes"., *J. Civil Eng. Mater. App*., **4**(4), 243-252. https://doi: 10.22034/jcema.2020.119979.

Fang, Q., Wang, G., Yu, F. and Du, J. (2021), "Analytical algorithm for longitudinal deformation profile of a deep tunnel", *J. Rock Mech. Geotech. Eng.*, **13**(4), 845-854. https://doi: 10.1016/j.jrmge.2021.01.012.

Fedrizzi, R.M., De Ceia, M.A.R., Misságia, R.M., Santos, V.H. and Neto, I.L. (2018), "Artificial carbonate rocks: synthesis and petrophysical characterization", *J. Petrol. Sci. Eng.*, **163**, 303-310. https://doi.org/10.1016/j.petrol.2017.12.089.

Gholami, S., Vafakhah, M., Ghaderi, K. and Javadi, M.R. (2020) "Simulation of rainfall-runoff process using geomorphology-based adaptive neuro-fuzzy inference system (ANFIS)". *Casp. J. Environ. Sci*., **18**(2), 109-122. https://doi: 10.22124/cjes.2020.4067.

Huang, H., Xue, C., Zhang, W. and Guo, M. (2022), "Torsion design of CFRP-CFST columns using a data-driven optimization approach", *Eng. Struct.*, **251**, p.113479. https://doi.org/10.1016/j. engstruct.2021. 113479.

Ivan'kova, Y.V. and Bogoslovskii, V.A. (2008), "Utilization of drill cuttings for interpretation of logging data in carbonate-rock oil and gas fields", *Moscow Univ. Geol. Bull.*, **63**(2), 128-130. https://doi: 10.3103/S0145875208020099.

Johansson, E., Miskovsky, K. and Loorents, K.J. (2009), "Estimation of rock aggregates quality using analyses of drill cuttings", *J. Mater. Eng. Perform.*, **18**(3), 299-304. https://doi.org/10.1007/s11665-008-9284-7.

Karaman, K. and Bakhytzhan, A. (2020), "Prediction of concrete strength from rock properties at the preliminary design stage", *Geomech. Eng.*, **23**(2), 115-125. https://doi.org/10.12989/gae.2020.23.2.115.

Klein, C. and Hurlbut, C.S. (1985), "*Manual of Mineralogy*", 20" ED.

Lee, M.Y., Ko, C.H., Chang, F.C., Lo, S.L., Lin, J.D., Shan, M.Y. and Lee, J.C. (2008), "Artificial stone slab production using waste glass, stone fragments and vacuum vibratory compaction", *Cement Concrete Compos.*, **30**(7), 583-587. https://doi.org/10.1016/j.cemconcomp.2008.03.004.

Lerman, N., Aronofsky, L. and Aghili, B. (2021), "Investigating the microstructure and mechanical properties of metakaolin-based polypropylene fiber-reinforced geopolymer concrete using different monomer ratios", *J. Civ. Eng. Mater. Appl*., **5**(3), 115-123. https://doi: 10.22034/jcema.2021.302140.1062.

Li, D., Liu, X. and Liu, X. (2015), "Experimental study on artificial cemented sand prepared with ordinary portland cement with different contents", *Mat*., **8**, 3960-3974. https://doi.org/10.3390/ma8073960.

Mateus, J., Saavedra, N.F. Calderón, Z.H. and Mateus, D. (2007), "Correlation development between indentation parameters and uniaxial compressive strength for Colombian sandstones", *CT&F-Ciencia Tecnología y Futuro*, **3**(3), 125-135. http://www.scielo.org.co/scielo.php?script=sci_arttext&pid=S0122-53832007000100008.

Mehrabi Mazidi, S., Haftani, M., Bohloli, B. and Cheshomi, A. (2012), "Measurement of uniaxial compressive strength of rocks using reconstructed cores from rock cuttings", *J. Petrol. Sci. Eng*., **86**, 39-43. https://doi.org/10.1016/j.petrol.2012.03.015.

Moradi, S.S.T., Nikolaev, N.I., Chudinova, I.V. and Martel, A.S. (2018), "Geomechanical study of well stability in high-pressure, high-temperature conditions", *Geomech. Eng*., **16**(3), 331-339. https://doi.org/10.12989/gae.2018.16.3.331.

Nes, O.M., Sønstebø, E.F. and Holt, R.M. (2001), *Rock Physics from Small Samples–Sometimes your only solution.* Extended abstract, SCA.

Singha, D. and Chatterjee, R. (2017), "Rock physics modeling in sand reservoir through well log analysis", Krishna-Godavari basin, India", *Geomech. Eng*., **13**(1), 99-117. https://doi.org/10.12989/gae.2017. 13.1.099.

Tilaki, G.A.D., Jolandan, M.A. and Gholami, V. (2020), "Rangelands production modeling using an artificial neural network (ANN) and geographic information system (GIS) in Baladeh rangelands, North Iran", *Casp. J. Environ. Sci.*, **18**(3), 277-290. https://doi.org/10.22124/CJES.2020.4139.

Wang, B., Liu, L., Wang, Y. and Li, L. (2020), "Stability evaluation of reinforced concrete structure of large coastal buildings", *J. Coast. Res.*, **103**(SI), 407-411. https://doi.org/10.2112/SI103-083.1.

Wang, Z., Wang, R. and Schmitt, D.R. (2015), *The Elastic Moduli of Velocities of Artificial Carbonate Rocks with Known Pore Structure at Different Saturation Conditions*. CSPG GeoConvention, March.

Xu, D., Liu, Q. and Qin, Y. (2021), "Analytical approach for crack identification of glass fiber reinforced polymer–sea sand concrete composite structures based on strain dissipations", *Struct. Health Monit*., 1475921720974290, https://doi: 10.1177/1475921720974290.

Xu, J., Zhou, L., Li, Y. and Ding, J. (2022) "Experimental study on uniaxial compression behavior of fissured loess before and after vibration", *Int. J. Geomech.*, **22**(2), p.04021277. https://doi: 10.1061/(ASCE)GM.1943-5622.0002259.

Yan, C., Deng, J., Cheng, Y., Yan, X., Yuan, J. and Deng, F. (2017), "Rock mechanics and wellbore stability in Dongfang 1-1 gas field in South China Sea", *Geomech. Eng.*, **12**(3), 465-481. https://doi.org/10.12989/gae.2017.12.3.465.

Zhang, S., Pak, R.Y. and Zhang, J. (2021), "Three-Dimensional Frequency-Domain Green's Functions of a Finite Fluid-Saturated Soil Layer Underlain by Rigid Bedrock to Interior Loadings", *Int. J. Geomech.*, **22**(1), p.04021267. https://doi.org/10.1061/(ASCE)GM.1943-5622.0002235.

Zhang, W. and Tang, Z. (2021), "Numerical modeling of response of CFRP–concrete interfaces subjected to fatigue loading", *J. Compos. Constr*., **25**(5), p.04021043. https://doi: 10.1061/(ASCE)CC.1943-5614.0001154.

GC